Structural Engineering and Mechanics, Vol. 32, No. 4 (2009) 531-547
DOI: http://dx.doi.org/10.12989/sem.2009.32.4.531

Central angle effect on connection behavior of steel box beam-to-circular column

Won-Sup Hwang†

Department of Civil Engineering, Inha University, 253 Yonghyun-Dong Nam-Gu, Incheon 402-751, Korea

Young-Pil Kim‡

Structural Department, Yooshin Engineering Corporation, 832-40 Yoksam-Dong, Gangnam-Gu, Seoul 135-936, Korea

Tae-Yang Yoon‡†

Steel Structure Research Lab., RIST, 79-5 Youngcheon, Dongtan, Hwasung, Kyunggido 445-813, Korea

(Received July 4, 2007, Accepted May 12, 2009)

Abstract. This paper presents the experimental results on the strength behavior and failure modes of box beam-to-circular column connections in steel piers. Previous research introduced parameters such as joint central angles, extension of horizontal stiffeners, and use of equivalent web depth, which ignored strength behavior and failure modes of box beam-to-circular column connections. The use of equivalent web depth d_2 is not reasonable when central angle α is closer to 90°; therefore, a monotonic loading test has been performed for eight connection specimens. From the test, it is identified that the connection with the circular column is stronger than the connection with the box-sectioned substitution column. Also, the strength of the beam-to-column connections with horizontal stiffeners is higher than the one of the no column stiffeners. The concrete-filled effect of box beam-to-circular column connection is also investigated, and the experimental yield strength of the connection is compared with the theoretical one. Also, more a reasonable equivalent web depth is suggested. The failure modes of connection are clearly defined.

Keywords: box beam-to-circular column connection; central angle; equivalent web depth; failure modes; concrete-filled; yield strength.

1. Introduction

Recently, steel piers have been widely applied for pier structures of urban overpasses and elevated structures in East Asian countries due to their small space requirements, excellent earthquake resistance capacity, and fast construction period. At the T-type or framed beam-to-column connections of box-

† Professor
‡ Ph. D. and P.E., Corresponding author, E-mail: feel75@hanmail.net
‡† Division Director

(a) box-sectioned frame type pier

(b) box-sectioned T type pier

(c) frame type pier with box beam and circular column connections.

Fig. 1 Beam-to-column connections of steel piers

sectioned steel piers as illustrated in Fig. 1(a) and Fig. 1(b), it has been widely acknowledged that serious shear lag and stress concentrations may occur due to abrupt direction changes in member forces, so it is necessary to handle these problems properly in the design stage. Instead of box-sectioned steel piers, as shown in Fig. 1(c), circular piers with box beam-to-circular column connections have been introduced recently due to a structural advantage of circular columns: they behave efficiently for a direction change of loading and they are a little affected by shear lag stress. Therefore, circular-sectioned piers are being recommended as a standard type of pier structures due to their external appearances. Researches on steel piers using circular-sectioned column have lately become a subject of special interest.

In an early study on welded steel connections, Beedle *et al.* (1951) proposed a stress and strength evaluation method for an H-sectioned beam-to-column connection by assuming that stresses are uniform in flanges and webs. Fielding and Huang (1971) indicated that the strength of the beam-to-column connection of a H-sectioned frame is reduced due to the axial force in the column. However, they did not recognize the shear lag phenomenon at the flange of connections. By recognizing the shear lag phenomenon at box-sectioned beam-to-column connections of the pier structure, Okumura and Ishizawa (1968) carried out theoretical and experimental studies using a simple beam model subjected to a concentrated mid-span load and, as a result, suggested an evaluation method for shear lag stresses. However, they overlooked a problem in assuming internal forces at the welded connection where the distribution of bending moments is closer to that of a cantilever beam rather than that of a simple beam. In addition, Okumura and Ishizawa (1968) did not consider the effective width of the flange plate seriously in estimating the shear lag and stress

concentration at the connection. Instead of using a simple beam model, Nakai *et al.* (1992) suggested an equation for the shear lag stress from a study using an overhanging beam model with additional moments due to shear deformation occurring in the connection. However, the result of Nakai *et al.* was also not much different from that of Okumura and Ishizawa. Recently, for connection of rolled sections, Popov and Takhiro (2002) experimented with two large bolted steel moment-resisting connections. Dubina and Stratan (2002) evaluated the behavior of different types of welds and of connections in terms of both performance and economical aspects. Also, Hwang *et al.* (2004) suggest shear lag stress evaluation method for box sectioned welded connection using the additional moment of cantilever beam model.

However, almost all researches, except Okumura and Ishizawa's, have been limited to box-sectioned connections only. Also, most researches do not consider that the behavior of the box beam-to-circular column connection is much more efficient than that of H-sectioned or box-sectioned connections in steel piers.

For the box beam-to-circular beam connection in steel piers, Okumura and Ishizawa (1968) performed an unique research through theoretical approaches. They suggested that the shear lag stress of circular column could be negligible and introduced the concept of equivalent web depth d_2 in the substitution of circular column. An equivalent web depth d_2 is the function of the central angle α, which is used to calculate the shear lag stress and shear stress of the box beam. However, d_2 has the problem that the shear lag stress and shear stress of the box beam was overestimated with the variation of the central angle α. Their study ignored failure modes of connections. The theoretical yield strength equations of box beam-to-circular column connection have not been suggested. Also, the experimental study of welded box beam-to-circular column connections has not been investigated sufficiently.

Therefore, in this research, monotonic loading tests are carried out for the eight beam-to-column connection models considering central angles, horizontal plate stiffeners, equivalent web depth, and the concrete-filled effect. From the results of out-of-plane deformation and strength of connection, failure modes and strength behavior are investigated. A more reasonable equivalent web depth is suggested, and the experimental yield strength of connection is compared with the theoretical one.

2. Test model

2.1 Model design

As shown in Fig. 2(a), L type specimens were prepared with corner parts of the circular-sectioned steel piers. In cases of box-sectioned connections, intersection regions of the beam and column are defined as the panel zone as shown Fig. 2(b). The panel zone of the box beam-to-circular column connection is defined using equivalent web depth d_2 of the circular column. Also, a span length-beam depth ratio L/d_b was fixed to about 4.0 because bending moment is more dominant than an axial force in the connection of steel piers (Nakai *et al.* 1982).

2.1.1 Central angle α

Based on the current design method, the equivalent web depth of the circular column could be calculated using equivalent web depth d_2 in the circular column-box beam connection. Thus, the circular column of may be substituted by the box-sectioned column as shown in Fig. 3(b).

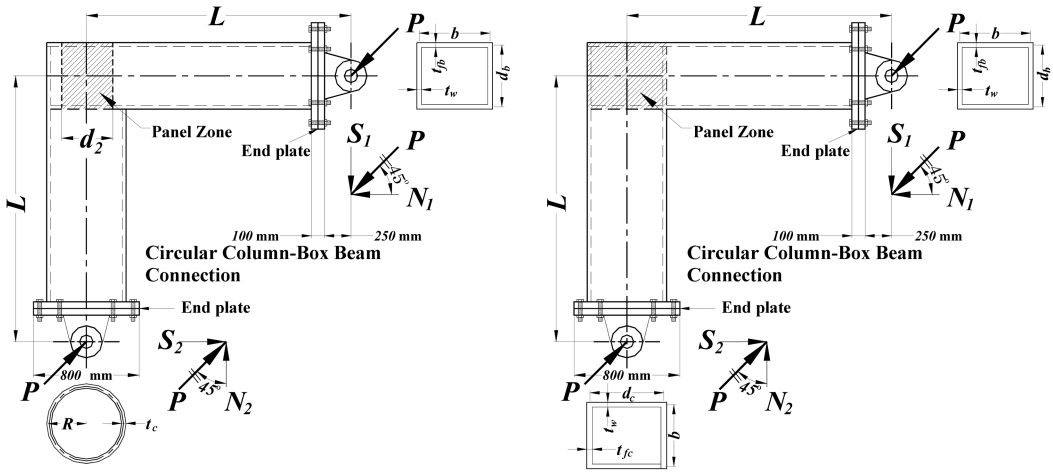

(a) box beam-to-circular column connection (b) box-sectioned connection

Fig. 2 Structural details of connection specimens

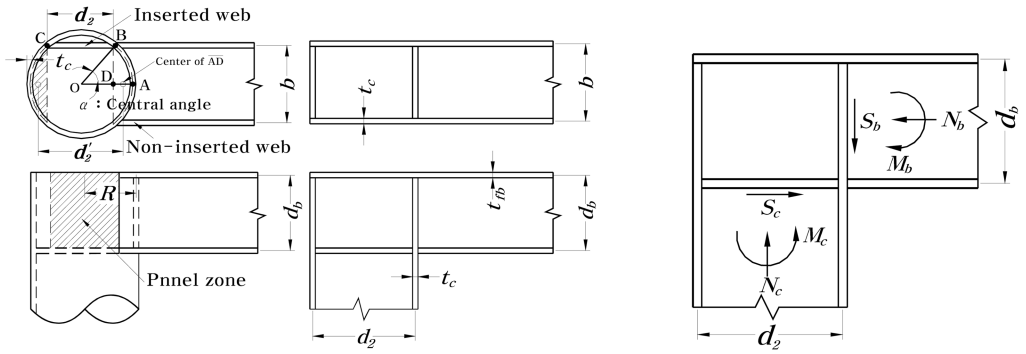

(a) Circular connection (b) equivalent web depth of connection (c) member forces at connection

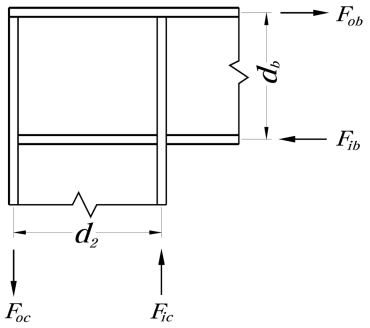

(d) flange concentration forces

Fig. 3 Definition of connection symbols

Equivalent web depth d_2 is used to calculate the shear lag stress of the lower flange of the beam and shear stress of the panel zone because flange concentration forces F of the circular section could not be calculated as shown in Fig. 3(c) and Fig. 3(d). Also, equivalent web depth d_2 is a function of central angle α (Fig. 3(a)). Central angle α limits the angle to a range between 45° to

55°, considering connection details from existing specifications (Meichi Highway Corporation 1984, Hanshin Highway Corporation 1985). Therefore, central angle α of specimens varies from 40° to 70° in this research. Also, test models of connection with equivalent web depth of the circular column were prepared to examine the adequacy of d_2.

2.1.2 Extension of horizontal stiffeners

In the structural details of the circular column-box beam connection, the web plate of the box-sectioned beam is usually welded to the circular column's surface. However, in the case of a column with thick web plates, the horizontal plate stiffeners could be extended into the inside of circular column (Hanshin Highway Corporation 1985).

2.1.3 Local buckling of plates

The radius-thickness ratio R/t_c of circular columns is about 25.0 in specimens. It is less than limitation values for the shear and compression of circular columns, where the limitation value for the shear is 40.0 (Hanshin Highway Corporation 1985) and the limitation value for compression is 50.0 (Korea Road Traffic Association 2005). Also, width-thickness ratio parameter R_f for the lower flange of box beam is defined as Eq. (1) (Korea Road Traffic Association 2005). R_f increase from 0.6 to 0.9 when the central angle varies from 40° to 70°.

$$R_f = \frac{b}{t_{bf}}\sqrt{\frac{12(1-v^2)}{4\pi^2}}\sqrt{\frac{f_{yf}}{E}} \tag{1}$$

in which, v, f_y, and E is Poisson's ratio of the steel (= 0.3), the yield stress of the flange plate, and Young's modulus of the steel, respectively.

2.1.4 Yielding moment ratio $M_y(v)/M_y(f)$

The deformation capacity of the connection varies with yielding type and failure mode of the connection. In general, as shown in Fig. 2(b), which is a box-sectioned connection, the yielding moment is defined as Eq. (2) when to the shear stress of the panel zone or the normal stress of the beam and column yields due to the use of the Von Mises' yield criteria (Hwang 1993).

$$M_y(v) = \frac{2t_w d_b d_c f_y}{\sqrt{3}}\left[\frac{1}{1-(d_b+d_c)/(2L)}\right] \tag{2a}$$

$$M_y(f) = \frac{f_y}{(1-d/(2L))/S+1/(AL)} \tag{2b}$$

In which, v is the shear stress of the panel zone and f is the normal stress of the beam and column.

When the yielding moment ratio $M_y(v)/M_y(f) \le 1.0$, the panel zone yielding occurs first. Also, by using d_2 instead of d_c in Eq. (2a), the shear yielding moment $M_y(v)$ of the box beam-to-circular column connection is derived as follows:

$$M_y(v) = \frac{2t_w d_b d_2 f_y}{\sqrt{3}}\left[\frac{1}{1-(d_b+d_2)/(2L)}\right] \tag{3}$$

Also, the yielding moment of the box beam lower flange is derived as Eq. (4a) by using R instead of $d/2$. The yielding moment of the circular column is derived as Eq. (4b). $M_y(f)$ should be chosen as minimum values between Eq. (4a) and Eq. (4b) when the yielding moment ratio $M_y(v)/M_y(f)$ is calculated.

$$M_{yb}(f) = \frac{f_y}{(1-R/L)/S_b + 1/(A_bL)} \tag{4a}$$

$$M_{yc}(f) = \frac{f_y}{(1-d_b/(2L))/S_c + 1/(A_cL)} \tag{4b}$$

in which, S_b and S_c is the sectional modulus of the beam and column, respectively. A_b and A_c are the sectional areas of the beam and column, respectively.

2.2 Dimensions of specimens

Table 1 shows each specimen's actual dimensions. The index N refers to non-concrete-filled connection, the next index C means the circular column-box beam connection, and next term is central angle α, respectively. Also, the equivalent web depth of the circular connection has the R index in the last term, and the model with the horizontal stiffener has S index in the last term.

Table 1 Dimensions of connection specimens

Model	α (deg.)	R (mm)	t_c (mm)	t_{fb} (mm)	t_w (mm)	d_b (mm)	d_2 (mm)	L (mm)	B (mm)	R/t	R_f	$M_y(v)/M_y(f)$
NC-40	40	290	11.83	11.83	11.83	485	444	1997	377	24.5	0.60	1.19
NC-45	45	291	11.82	11.82	11.82	486	410	1995	416	24.6	0.67	1.09
NC-50	51	286	11.91	11.91	11.91	484	359	1994	445	24.1	0.72	0.94
NC-55	56	287	11.81	11.81	11.81	486	320	1991	486	24.2	0.78	0.83
NC-60	60	292	11.86	11.86	11.86	486	293	1995	504	24.6	0.81	0.75
NC-70	69	293	11.88	11.88	11.88	488	212	1995	547	24.7	0.89	0.53
NC-45R	56	289	11.85	11.85	11.85	486	322	1993	490	24.4	0.79	1.28
NC-55S	–	–	11.86	11.86	11.86	488	418	1999	415	–	0.67	1.28

Notation :

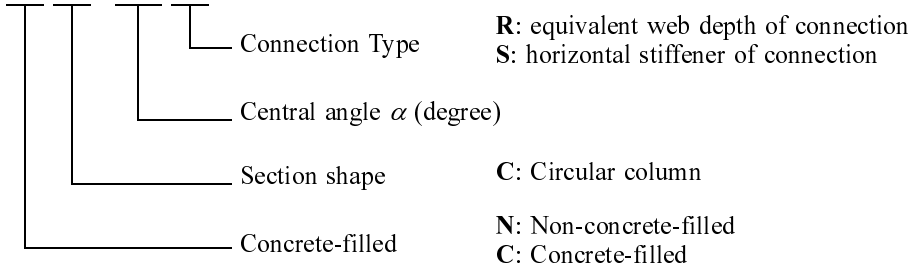

Table 2 Mechanical properties of materials

f_y (MPa)	f_u (MPa)	E ($\times 10^5$ MPa)	f_y/f_u	Steel Class
286	464	1.9992	0.62	SS400

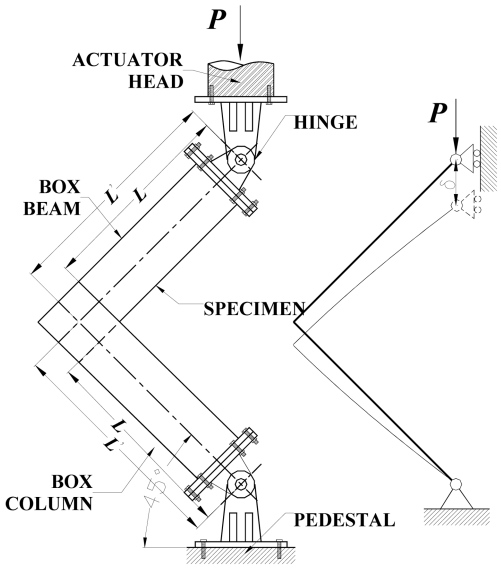

Fig. 4 Test setup and boundary condition

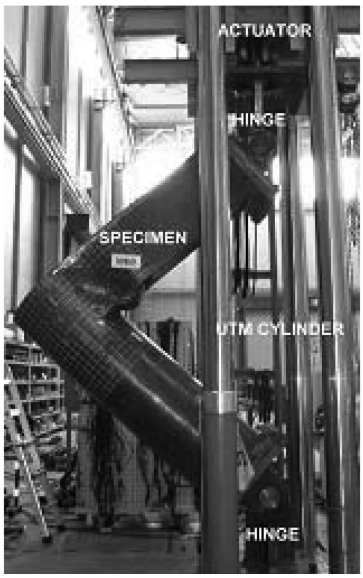

Fig. 5 Side view of test device

Notation of the specimens is expressed as follows.

Also, eight tensile test specimens of materials are made from type KS B 0801 No. 1. As shown in Table 2, lower yield stress f_y and tensile stress f_u is satisfied with standard stress, where standard yield stress f_y should be over 235 MPa and an allowable range of standard tensile stress f_u is from 402 to 510 MPa in SS400 class steel (Korea Road Traffic Association 2005).

2.3 Test setup and method

2.3.1 Test setup

Figs. 4 and 5 show the test setup and a side view of the connection. Both edges of the specimen were supported by hinges. The lower hinge was fixed by using a high-tension bolt with a pedestal. Vertical displacement of the upper hinge was free because upper hinge was connected to the actuator of UTM, The capacity of the loading device was ±3000 kN, and the maximum stroke of cylinder was ±300 mm. To measure the out-of-plane deformation of the lower flange of the beam and circular column compression part, studs were installed in each plate center, in which the clearance from the welding line to the studs was 150 mm. By using piano wire, each stud was connected to the LVDT (100 mm), which was attached to the end plate. Also, at the center of the panel zone and box beam web, 50 mm of dial gauge was installed with normal direction of the surface. To measure the shear deformation of connection, two 100 mm LVDTs were installed diagonally at the connection curved panel zone.

2.3.2 Test method

In the steel pier connection, negative moment generally occurs due to the vertical load; therefore, L type connection is introduced as shown Fig. 4, so that compression force is exerted on the lower flange of the box beam. Displacement control loading method is used with the speed of 1 mm/min. Monotonic loading is increased until the connection collapses, as shown in Fig. 5.

3. Test results

3.1 Load-displacement relationship of connection

3.1.1 Influence of central angle α

Fig. 6 shows load P and vertical displacement δ relationships with central angle α. Each arrow mark means yield strength P_o and ultimate strength P_u. From this figure, the strength of connections is classified into three categories with central angle α; i.e., in the case of the NC-40 model, in which central angle α is 40°, strength increases slowly after yielding. It reaches maximum strength at 65 mm displacement. After maximum strength, strength reduced slowly until 100 mm displacement and reduced rapidly after 100 mm displacement. In the case of NC-45, NC-50, and NC-55 models, their strength is more stable than that of NC-40. After reaching maximum strength, strength reduction is minimal. In the case of NC-60 and NC-70 models, after maximum strength, immediate strength reduction occurred but strength reduced slowly.

3.1.2 Influence of equivalent web depth and extension of horizontal stiffeners

Previously in Chapter 2.1.1, substitution from the circular section to the box section is explained using equivalent web depth d_2. Fig. 7 shows the relationship between load P and displacement δ of the substituted model (NC-45R) and web inserted model (NC-55S). The yield strength P_o of the NC-45R model is much less than that of the NC-45 model. Maximum strength P_u of the NC-45R model is smaller than the NC-45 model. Also, the behavior of the NC-45 and NC-45R models differs greatly after ultimate strength. Therefore, it was suggested that the failure mode of the connection should be considered in the case of the substituted connection using equivalent web depth d_2. The strength of NC-55S increases about 12% compared with the strength of NC-55. However, because the strength of the NC-55S model decreases rapidly after maximum strength, the NC-55S model has low deformation capacity. Therefore, these results support the idea that the extension of horizontal stiffeners is inefficient due to complicated fabrication procedures as well as low deformation capacity.

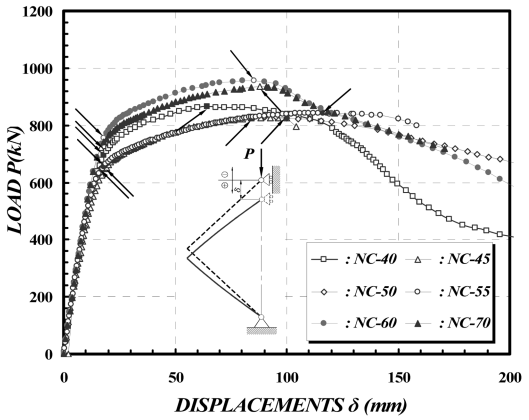

Fig. 6 Influence of central angle α

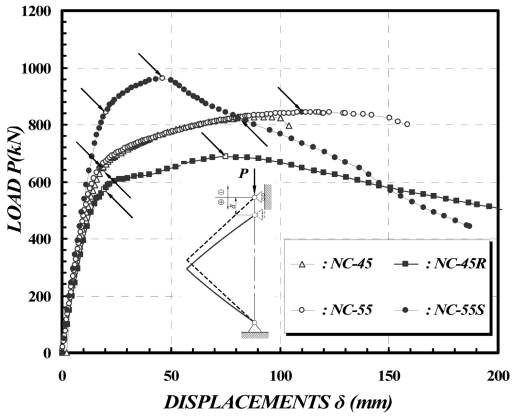

Fig. 7 Influence of equivalent web depth and extension of horizontal stiffeners

3.2 Out-of-plane deformation of plates

Fig. 8 shows out-of-plane deformation of representative specimens, which are NC-40, NC-50, and NC-60; in these cases, a plus sign (+) means convex out-of-plane deformation of plates and a minus sign (−) means concave out-of-plane deformation of plates. Out-of-plane deformation δ_{bf} of the beam lower flange increases with increase of central angle α. However, out-of-plane deformation δ_c of the column compression part decreases with an increase of central angle α. In the case of the NC-40 model, out-of-plane deformation δ_{bf} of beam lower flange is constant after maximum strength but δ_c of column increases significantly. The strength reduction of the connection occurred rapidly due to column deformation. The NC-60 model shows the opposite trend of out-of-plan deformation comparing with the NC-40 model. The strength of the connection decreases due to a large increase of δ_{bf}. Also, the NC-50 model behaves stable comparing with other models because δ_{bf} and δ_c of the NC-50 model occurred simultaneously.

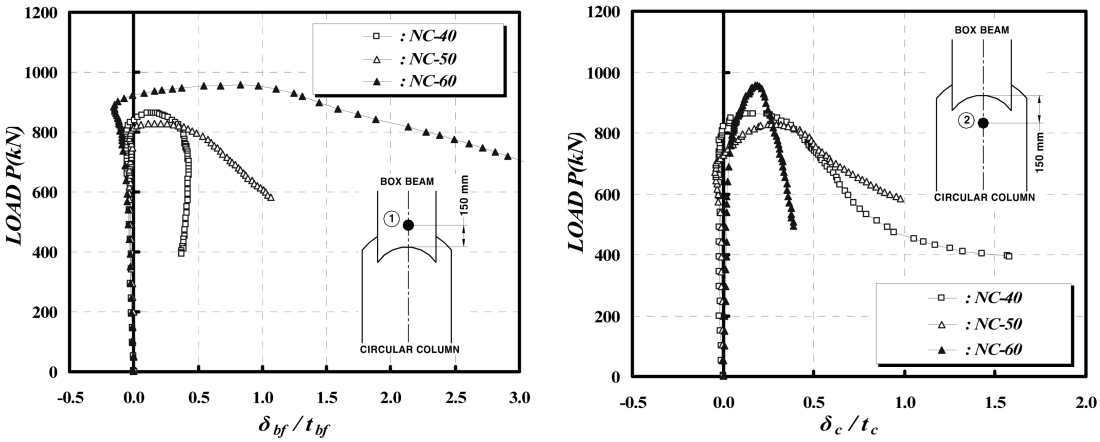

(a) beam lower flange (b) inside of circular column.

Fig. 8 Out-of-plane deformation of plates

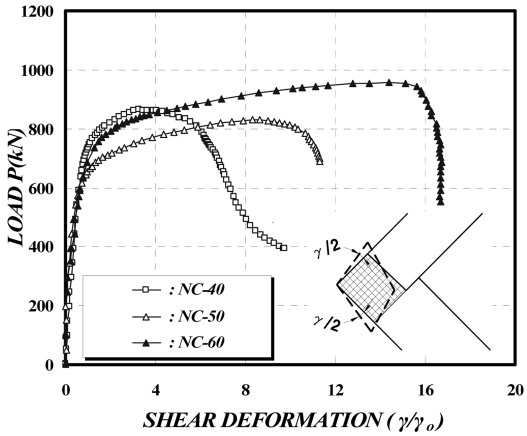

Fig. 9 Load P shear deformation γ/γ_0 relationship of curved panel zone

3.3 Shear deformation of the panel zone

Fig. 9 shows the load P shear deformation γ/γ_o relationship of the curved panel zone. Shear deformation γ of the panel zone was obtained by assuming the curved panel to be a straight panel because the shear deformation of a curved panel is difficult to measure. Shear deformation γ is normalized by yield shear deformation γ_o based on P_o. Shear deformation γ/γ_o of the panel zone increases remarkably with an increase in central angle α. In case of a small α region such as the NC-40 model, strength increase slowly after ultimate strength; however, in the 60^o and over region, maximum strength was affected by increases in the shear deformation due to the rapid reduction of the panel zone area.

3.4 Failure modes

From the final deformation shapes of this experiment, the failure modes of box beam-to-circular column connections were classified by three categories as follows.

3.4.1 Column buckling type

Fig. 10(a) shows the column buckling type of box beam-to-circular column connections. In the initial loading stage, out-of-plane deformation increases slowly in the lower flange of the beam and column compression part; however, the out-of-plane deformation of the column compression part increases, so the connection is collapsed due to the deformation of the internal diaphragm of the column. In this paper, the NC-40 model was included in this failure type. Also, this type is the most disadvantageous failure type considering the strength and the deformation capacity of the box beam-to-circular column connection.

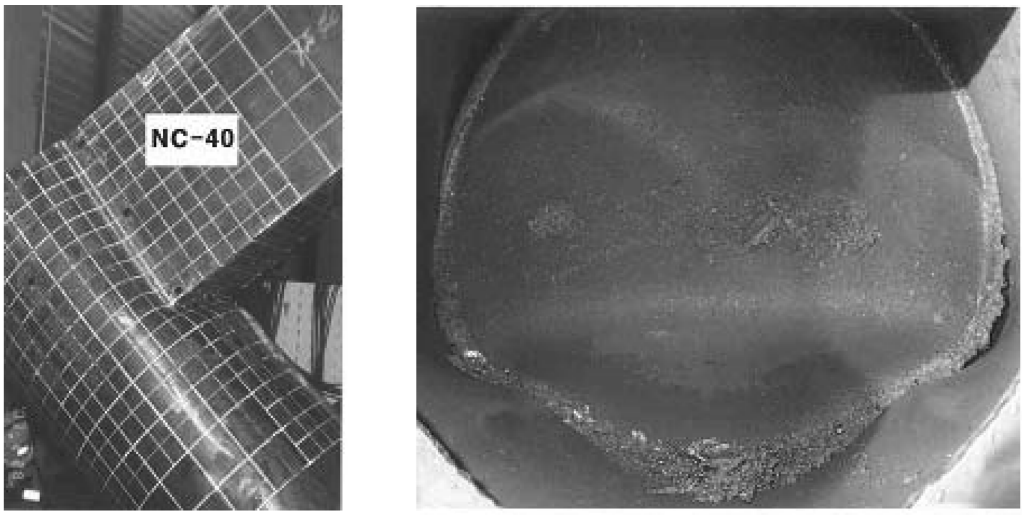

(a) buckling of column (b) buckling of internal diaphragm

Fig. 10 Column buckling type

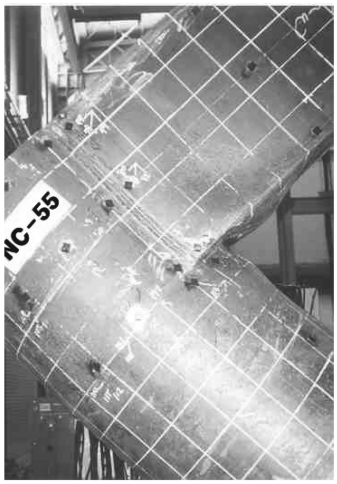

Fig. 11 Beam & column buckling type

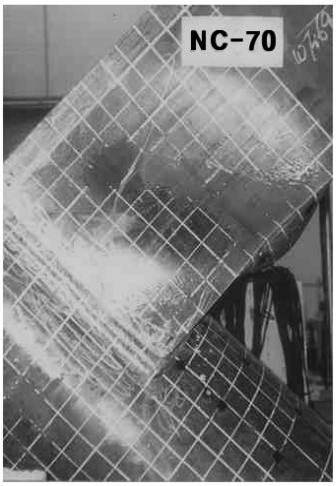

Fig. 12 Beam buckling type

3.4.2 Beam and column buckling type

Fig. 11 shows the beam and column buckling type of box beam-to-circular column connections. In this failure type, out-of-plane deformation of the lower flange of the box beam increases until reaching ultimate strength. After ultimate strength, the internal diaphragm buckles. Then, the connection collapses owing to the out-of-plane deformation of the compression part of the column. The deformation of the beam and column was not concentrated at any point. Also, the region occurring out-of-plane deformation changes from the lower flange of the beam into column compression part with increase of loading steps. In this paper, NC-45, NC-50, and NC-55 models are included with this type.

3.4.3 Beam buckling type

Fig. 12 shows the beam buckling type of box beam-to-circular column connection. In this failure type, out-of-plane deformation is concentrated at the lower flange of the beam. Out-of-plane deformation of internal diaphragm and column compression part did not occur. Following ultimate strength, strength reduction is observed immediately, but out-of-plane deformation of the lower flange of the beam is prevented due to the tension field effect of the web plate of the beam as shown in Fig. 12. Therefore, strength reduction of this failure type occurs slowly. In this paper, NC-60 and NC-70 models are classified into the beam buckling type.

3.5 Comparison with concrete-filled connection

3.5.1 Strength behavior

To compare with the strength behavior of the concrete-filled box beam-to-circular column connections, six concrete-filled connection specimens (CC models) which have equal dimensions to NC-40 to NC-70 were prepared. Yield strength P_o is obtained from the test as shown in Fig. 13 (Lee and Lui 1989); i.e., P_o and d_o are defined at the intersection point of K_o line and $K_o/10$ line. Concrete was completely filled in the inner part of panel zone as well as the section of the beam and column. Also, they were loaded as the same test method of the NC model. Fig. 14 shows load

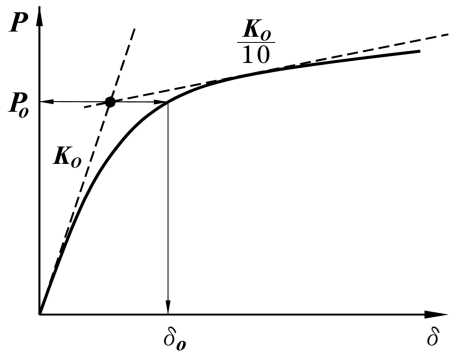

Fig. 13 Definition of P_o

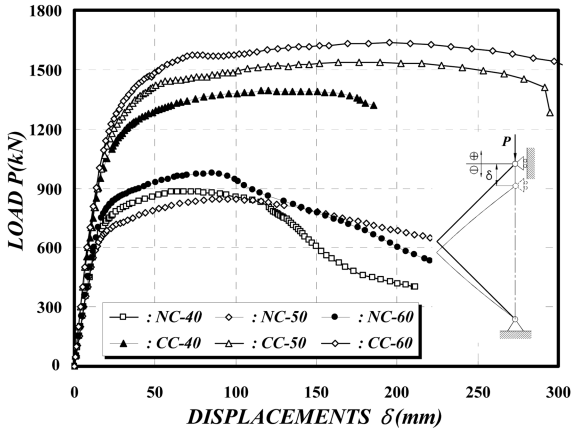

Fig. 14 Comparison with concrete-filled connections

P and Displacement δ relationship of the NC and CC model. The yield strength of the CC model is much stronger than that of the NC model by about 1.58 to 1.93 times. Also, the ultimate strength of the CC model is much stronger than that of the NC model by about 1.61 to 1.82 times. This phenomenon occurs due to confined effect and compression strength of concrete. The deformation capacity of the CC model is much larger than that of the NC model because the CC model maintains the strength after 100 mm of displacement. Although strength behavior of the CC model differs from one of the NC model, a sufficient design method using a concrete-filled connection has not been designed yet. Also, concrete-filled box beam-to-circular column connections have not reached the stage of practical use. Therefore, further study on the strength behavior of concrete-filled connections is needed to determine the cause of this discrepancy.

3.5.2 Failure modes

As shown in Fig. 15, failure modes of the concrete-filled box beam-to-circular column connection are classified into two categories as follows: in the case of the beam buckling type, as shown in

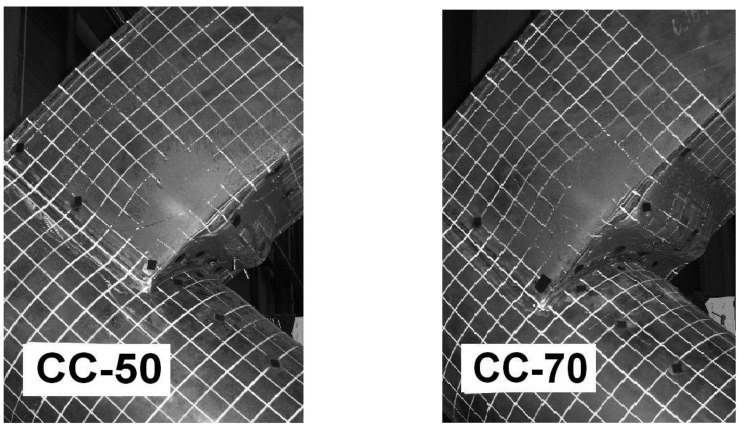

(a) beam buckling type (b) beam and column buckling type

Fig. 15 Failure modes of concrete-filled connection

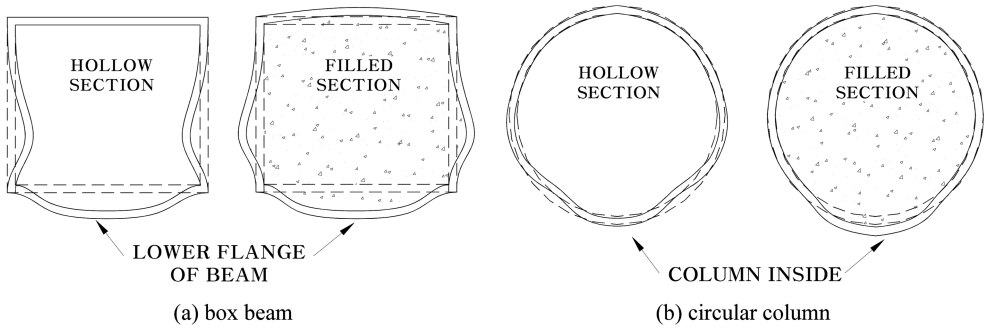

Fig. 16 Comparison of deformation shape

Fig. 15(a), out-of-plane deformation is concentrated at the beam lower flange of concrete-filled connections with a small central angle such as CC-40, CC-45, and CC-50. In the case of the beam and column buckling type as shown in Fig. 15(b), Out-of-plane deformation of beam and column of concrete-filled connections were not concentrated at any point. Also, Fig. 16 shows the deformation of the connection. The web of the box beam of the concrete-filled connection deforms in the reverse direction comparing with non-concrete-filled connection. The severe deformation of the non-concrete-filled circular column occurred due to the punching by the web of the box beam.

4. The strength and yielding type of connection

4.1 Yield strength

By considering Eq. (3) and equivalent web depth d_2 instead of d_c, the yield strength $P_y(v)$ of the panel zone is derived as expressed in Eq. (5a).

$$P_y(v) = \frac{2\sqrt{2}t_w d_b d_2 f_y}{\sqrt{3}L}\left[\frac{1}{1-(d_b+d_2)/(2L)}\right] \tag{5a}$$

For the normal stress of the beam and column, by substituting radius R of the circular column, sectional area ratio S_b of the beam, and beam area A_b, in Eq. (4a), yield strength $P_{yb}(f)$ of beam is derived as shown in Eq. (5b).

$$P_{yb}(f) = \frac{\sqrt{2}f_y}{(L-R)/S_b + 1/A_b} \tag{5b}$$

Similarly, by considering web depth d_b of box beam, sectional area ratio S_c of column, column area A_c, and Eq. (4b), yield strength $P_{yc}(f)$ of the circular column is derived as follows.

$$P_{yc}(f) = \frac{\sqrt{2}f_y}{(L-d_b/2)/S_c + 1/A_c} \tag{5c}$$

Table 3 shows the test results of the specimens. As shown in Table 3, P_o of NC-40 differs by 6% from the theoretical yield strength $P_{yb}(f)$ and $P_{yc}(f)$. When the diaphragm yielding of the circular column compression parts occurs first, the theoretical yield strength using Eq. (5) has a difference

Table 3 Test results

Specimens	Test results			Theoretical value				
				$P_o/P_y(v)$			$P_o/P_{yb}(f)$	$P_o/P_{yc}(f)$
	P_o (kN)	P_u (kN)	P_u/P_o	d_2	d_2'	d_e^*	$P_o/P_{yb}(f)$	$P_o/P_{yc}(f)$
NC-40	697	864	1.24	0.89	0.76	0.88	1.06	**1.06**
NC-45	643	826	1.28	0.90	0.72	0.82	0.91	**0.98**
NC-50	647	829	1.28	1.06	0.79	0.86	0.88	**0.99**
NC-55	652	844	1.29	1.20	0.83	0.87	0.82	**1.00**
NC-60	760	956	1.26	1.55	**0.99**	**1.02**	0.93	1.16
NC-69	721	935	1.30	2.07	**1.04**	**0.99**	0.83	1.10
NC-45R	572	687	1.20	0.78	-	-	0.84	**1.00**
NC-55S	843	961	1.14	-	-	-	1.28	1.29

*$d_e = 2R/\pi + R\sin(\alpha)/\alpha$

with experimental one. In the case of the central angle from 45° to 55°, P_o agrees well with the yield strength by using Eq. (5b). Thus, Eq. (5) gives the exact yield strength of the connection when local buckling of the column does not occur in the central angle from 45° to 55°. Also, when the central angle is greater than 60°, yield strength P_o agrees well with the yield strength of the panel zone based on d_e. In Chapter 3.4, the strength of specimens varies greatly after ultimate strength. However, the strength ratio (P_u/P_o) of all specimens is constant around 1.25.

4.2 Classification of yielding type

The yielding type of connection has an effect on failure modes of the connection. The yielding type of connection could be sorted by comparing the theoretical yield strength. In general, the yielding type of connection is the beam yielding type and column yielding type; however, the yield strength of a connection considering diaphragm yielding has been ignored. Also, a panel zone yield

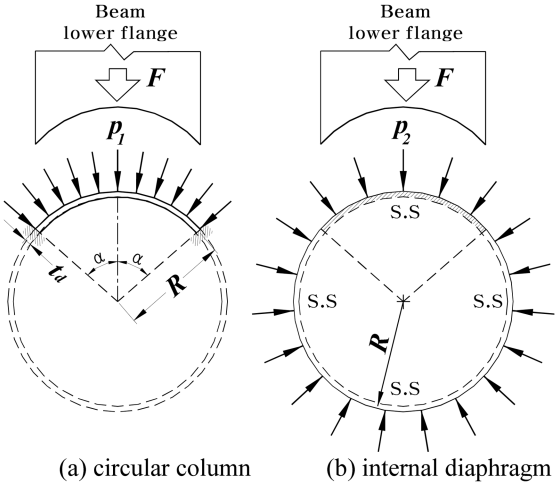

(a) circular column (b) internal diaphragm

Fig. 17 Model of internal diaphragm

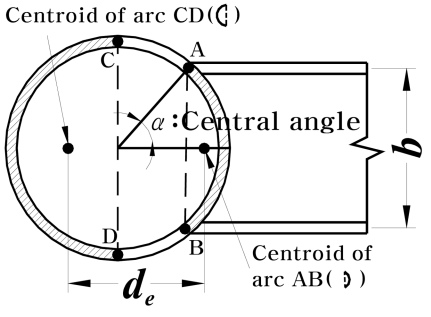

Fig. 18 Effective web depth d_e

strength $P_y(v)$ changes remarkably with the equivalent web depth d_2 or d_2'; Therefore, the circular column is assumed, as shown in Fig. 17(a), to be an arch with a central angle 2α. It is subjected to uniform load p_1 due to hoop effect of circular column and diaphragm which is induced by concentration force F of the lower flange of the beam. Boundary condition of circular column is assumed to be fixed ends and buckling load of circular column is $p_{1(cr)}$. Also, as shown in Fig. 17(b), uniform load p_2 is induced from the uniform reaction force of the normal force with radial ones. Boundary condition of diaphragm is assumed to be all simply supported ends and buckling load of internal diaphragm is defined as $p_{2(cr)}$. The yield strength $P_{yd}(f)$ of the diaphragm of the circular column is derived as Eq. (6) because flange concentration force F is obtained by multiplying arc length ($=2\alpha R$) and diaphragm thickness t_d. Also, as shown in Fig. 18, equivalent web depth d_e is defined as the distance from the centroid of arc CD to the centroid of arc AB. $P_y(v)$ could be calculated by using d_e with central angle α.

$$P_{yd}(f) = \frac{2\sqrt{2}\,\alpha R\cos(\alpha/2)t_d(p_{1(cr)}+p_{2(cr)})}{(L-R)/d_b+1/2} \tag{6}$$

where t_d is thickness of diaphragm and $p_{1(cr)}$, $p_{2(cr)}$ are defined as followings (Walter 1994).

$$p_{1(cr)} = \left(0.14+\frac{3.2}{\lambda^2}\right)K_c \tag{7a}$$

$$p_{2(cr)} = \frac{0.8E}{\sqrt{1-\nu^2}}\left(\frac{t_d}{R}\right)^2 \tag{7b}$$

where K_c, and λ is defined as followings (Walter 1994).

$$K_c = \frac{2}{\sqrt{3(1-\nu^2)}}E\left(\frac{t_d}{R}\right)^2 \tag{8a}$$

$$\lambda = [12(1-\nu^2)]^{1/4}\sqrt{\frac{R}{t_c}}\left(2\sin\left(\frac{\alpha}{2}\right)\right) \tag{8b}$$

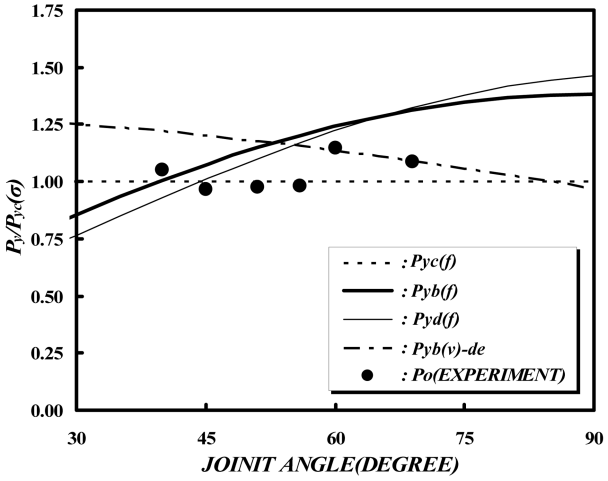

Fig. 19 Yielding type of connections

Fig. 19 shows the normalized yield strength P_y/P_{yc} and central angle α relationships of the specimens. In the range which the central angle v is less than 45°, the diaphragm yielding occurs first. Specially, as the central angle α equals 40°, the yield strength increases due to the stiffening effect of the diaphragm. When α is from 50° to 55°, the connection is classified as the column yielding type. When the local buckling of the lower flange of the beam occurs, column and beam yield simultaneously. Also, when the range central angle α is over 60°, the yield strength increases due to the hoop effect of the diaphragm. The curved panel zone of the box beam-to-circular column connection yields due to the rapid reduction of the panel zone area with central angle α.

5. Conclusions

This paper summarizes the test results of strength behavior and failure modes of connections to develop the design method of steel piers. From this study, the following conclusions can be drawn:

(1) Three types of the strength behavior of the circular column-box beam connection are classified with different central angle α. The range in which a central angle is less than 55° over 45° is the most profitable type of connection in the strength and deformation capacity aspect.

(2) The strength of connections using equivalent web depth d_2 is much less than one of the box beam-to-circular column connection. The strength and deformation capacity changes remarkably due to the difference of the failure type. Therefore, the method of the equivalent web depth, d_e, of connections is suggested.

(3) The strength of the connections with the extension of horizontal stiffeners was reduced remarkably after reaching ultimate strength. This connection is not efficient in view of the deformation capacity and manufacturing difficulty.

(4) With the increase of central angle α, out-of-plane deformation δ_{bf} of the lower flange of the beam increases, but out-of-plane deformation δ_c of the compression part of the column decreases.

(5) The strength of the concrete-filled model is much stronger than one of the NC model, about 1.61 to 1.82 times, due to the prevention of plate local buckling by the concrete confined effect. The deformation capacity of the CC model is much larger than that of the NC model because CC models maintain their strength after 100 mm displacement.

(6) Failure modes of the circular column-box beam connection are defined as column buckling, beam - column buckling, and beam buckling with central angle α. The beam - column buckling type was more profitable in the strength and deformation of the connection. Failure mode of the concrete-filled circular column-box beam connection are classified into beam buckling and beam - column buckling.

(7) The box beam web of the concrete-filled connection deforms in an opposite direction compared with that of the non-concrete-filled connection. Also, the deformation of the non-concrete-filled circular column occurred greatly due to the punching from the web of the box beam.

(8) When central angle α is less than 45°, the diaphragm of the internal circular column yielded first. When central angle α is over than 60°, the panel zone yielded due to rapid reduction of the panel zone area.

References

Beedle, L.S., Topractsoglou, A.A. and Jonhston, B.G. (1951), "Connection for welded continuous portal frames", *Welding J.*, **30**, 354s-384s.

Dubina, D. and Stratan, A. (2002), "Behavior of welded connections of moment resisting frames beam-to-column joints", *Eng. Struct.*, **24**, 1431-1440.

Fielding, D.J. and Huang, J.S. (1971), "Shear in steel beam-to-column connections", *Welding J.*, **50**(7), 313s-326s.

Hanshin Highway Corporation (1985), *Design Standard. No. 2: Design of Structure (part of bridge)*.

Hwang, W.S., Kim, Y.P. and Park, Y.M. (2004), "Evaluation of shear lag parameters for beam-to-column connections in steel piers", *Struct. Eng. Mech.*, **17**(5), 691-706.

Hwang, W.S. (1993), "Inelastic behavior and provisions for limit state design of beam-to-column connections in steel bridge pier structures", *Ph.D. thesis*, Osaka University of Japan.

Kawai, J., Furukawa, K. and Hayashi, H. (1979), *The Design and Solutions of Steel Pier*, Rikou Books (in Japanese).

Korean Road Traffic Association (2003), *Road Bridge Design Specifications*.

Lee, S.J. and Lu, L.W. (1989), "Cyclic tests of full scale composite joint sub-assemblages", *J. Struct. Eng.*, ASCE, **115**(8), 1977-1998.

Luo, Q.Z., Tang, J. and Li, Q.S. (2002), "Experimental studies on shear lag of box girder", *Eng. Struct.*, **24**, 464-477.

Meichi Highway Corporation (1984), *Design Standard of Steel Structure* (in Japaneses).

Nakai, H., Kitada, S., Kawai, J., Miki, T. and Yoshikawa, O.A. (1982), "Investigations of steel piers construction examples - I, II", *Bridges Found.*, 35-49 (in Japanese).

Nakai, H., Miki, T. and Hashimoto, Y. (1992), "On limit state design method considering shear lag phenomenon of corner parts of steel rigid frames", *JSCE*, **455**, 95-104 (in Japanese).

Okumura, T. and Ishizawa, N. (1968), "The design of knee joints for rigid steel frames with thin walled section", *JSCE*, **153**, 1-17 (in Japanese).

Popov, E.P. and Takhirov, S.M. (2002), "Bolted large seismic steel beam-to-column connections Part 1: Experimental study", *Eng. Struct.*, **24**, 1524-1534.

Walter, D. Pilkey (1994), *Stress, Strain, and Structural Matrices*, Johnwiley and Sons.